

Closed-Loop Verbal Reinforcement Learning for Task-Level Robotic Planning

Dmitrii Plotnikov*, Iaroslav Kolomiets*, Dmitrii Maliukov*, Dmitriij Kosenkov, Daniia Zinniatullina, Artem Trandofilov, Georgii Gazaryan, Kirill Bogatikov, Timofei Kozlov, Igor Duchinskii, Mikhail Konenkov, Miguel Altamirano Cabrera and Dzmitry Tsetserukou

Abstract—We propose a new Verbal Reinforcement Learning (VRL) framework for interpretable task-level planning in mobile robotic systems operating under execution uncertainty. The framework follows a closed-loop architecture that enables iterative policy improvement through interaction with the physical environment. In our framework, executable Behavior Trees are repeatedly refined by a Large Language Model actor using structured natural-language feedback produced by a Vision-Language Model critic that observes the physical robot and execution traces. Unlike conventional reinforcement learning, policy updates in VRL occur directly at the symbolic planning level, without gradient-based optimization. This enables transparent reasoning, explicit causal feedback, and human-interpretable policy evolution. We validate the proposed framework on a real mobile robot performing a multi-stage manipulation and navigation task under execution uncertainty. Experimental results show that the framework supports explainable policy improvements, closed-loop adaptation to execution failures, and reliable deployment on physical robotic systems.

I. INTRODUCTION

In real-world environments, mobile robots operate under significant execution uncertainty [1]. Variations in layouts, imperfect localization, and low-level control errors make the design of robust task-level policies challenging and time-consuming [2]. In practice, such policies are often implemented using Behavior Trees (BTs), which provide modularity and transparency but require significant manual tuning to handle unexpected failures [3], [4].

Reinforcement learning (RL) offers a principled framework for autonomous policy improvement through interaction and iteration. However, most RL approaches optimize policies in a sub-symbolic space, producing behaviors that are difficult to interpret or debug [5]. This lack of transparency limits their applicability for the real-world deployment of robotic systems.

Recent work [6], [7], [8], [9], [10] has explored the use of large language models (LLMs) for robotic task planning, leveraging their reasoning and generalization capabilities [11], [12]. While promising, LLM-based planners typically operate in an open-loop manner and lack grounded feedback

*These authors contributed equally to this work.

The authors are with the Intelligent Space Robotics Laboratory, Skolkovo Institute of Science and Technology. {dmitrii.plotnikov2, iaroslav.kolomiets, dmitrii.maliukov, dmitriij.kosenkov, daniia.zinniatullina, artem.trandofilov, georgii.gazaryan, kirill.bogatikov, timofei.kozlov, igor.duchinskii, mikhail.konenkov, m.altamirano, d.tsetserukou}@skoltech.ru

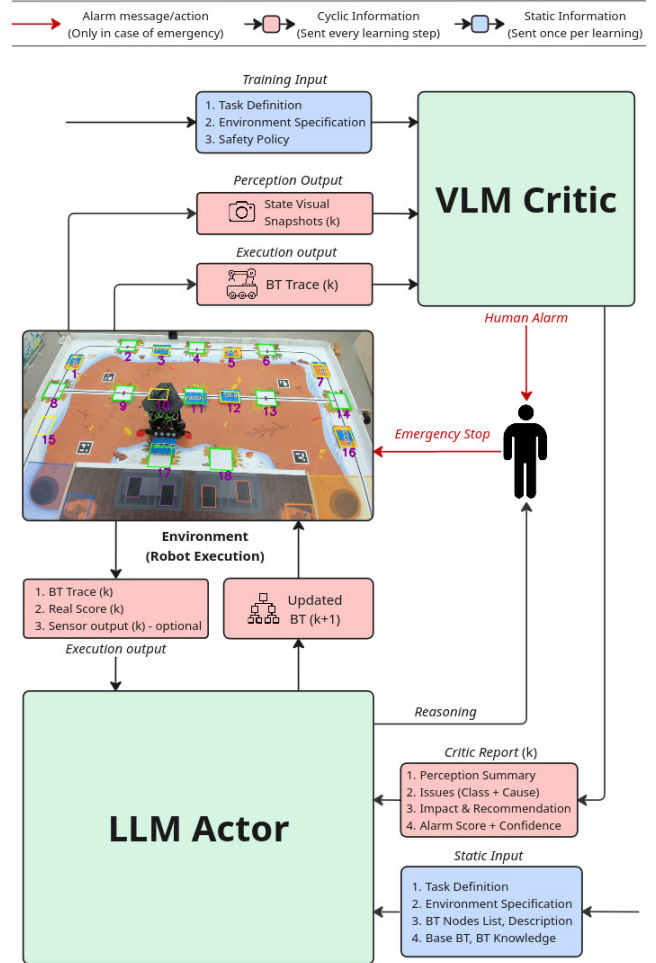


Fig. 1. System architecture.

from the physical world. As a result, they struggle to reliably adapt to real-world execution failures.

To address these limitations, we propose a closed-loop Verbal Reinforcement Learning (VRL) framework for task-level robotic planning. In VRL, task policies are represented as executable Behavior Trees and iteratively refined through structured natural-language feedback. An LLM-based actor modifies the task plan, while a vision-language model (VLM) critic analyzes robot operation using visual observations and execution traces [13]. Unlike prior work, VRL explicitly

separates causal diagnosis (critic) from symbolic policy modification (actor), enabling hardware-aware adaptation without gradient-based learning.

II. RELATED WORK

Recent advances in large foundation models have significantly influenced robotic perception, planning, and decision-making. Large language and vision–language models become more common in robotic systems as they allow for more flexible and adaptable control of the robots.

A. LLMs for Task-Level Planning and Code Generation

Recent works employ large language models as high-level planners that translate natural-language instructions into executable code or symbolic task plans. Some systems [14], [15], [16], [17], [18], [19] combine LLM-based common sense reasoning with task-and-motion planning, converting underspecified goals into commands that can be executed by classical planners. These approaches demonstrate strong semantic reasoning, but they typically operate in a one-shot or open-loop manner and lack systematic mechanisms for strategy refinement.

BTs provide an interpretable and modular representation for LLM-driven planning. Previous research showed that LLMs can synthesize structurally valid BTs from natural-language commands [20]. However, existing approaches focus primarily on initial plan generation and do not address post-deployment policy improvement.

B. Vision–Language Models for Reward Learning and Evaluation

Vision–language models have been widely explored for reward learning in robotics. Some methods [21], [22], [23], [24], [25] derive preference-based rewards from visual comparisons, providing automated supervision for reinforcement learning. These approaches rely on gradient-based optimization in sub-symbolic policy spaces, limiting their interpretability. Other works employ VLMs for affordance extraction or scene understanding, primarily as perception modules rather than explicit execution critics.

C. Critic-Based Policy Refinement

Recent studies investigate VLMs [26], [27] as behavioral critics that identify undesirable or unsafe actions and support iterative refinement. However, prior methods typically evaluate or rank policies without directly modifying structured symbolic representations such as Behavior Trees.

In contrast, our work couples a VLM-based visual critic with an LLM actor that performs direct, interpretable updates of executable Behavior Trees. This enables closed-loop task-level policy refinement on a physical robot without gradient-based reward learning or simulation.

III. VERBAL RL FRAMEWORK FOR TASK-LEVEL ROBOTIC PLANNING

This section formalizes our framework and describes the actor–critic interaction, symbolic policy representation, and execution-driven refinement mechanism.

A. Policy Representation

Task policies are represented as executable Behavior Trees (BTs), which provide modularity and interpretability.

The actor modifies BT structure and parameters directly, operating on a library of predefined human-designed nodes and subtrees. This allows policy updates to remain transparent, verifiable, and grounded in existing expert knowledge. The initial BT is deliberately simple and does not encode task strategy, serving only as a basis for iterative improvement.

B. LLM Actor: Symbolic Policy Refinement

The actor is an LLM that operates at the symbolic level, refining an existing BT based on structured feedback. To constrain the search space and ensure syntactic validity of generated policies, the actor is prompted with a structured context consisting of: (i) the task definition, (ii) an environment specification, (iii) a library of available BT nodes with their descriptions, and (iv) BT authoring knowledge (coding rules) together with the current (initial) BT. Importantly, the actor does not receive raw sensory streams and does not directly control the robot; instead, it proposes discrete, interpretable edits to the BT structure and parameters.

Optionally, the actor’s input interface can be augmented with additional structured, perception- or sensor-derived state estimates when available. We treat this as an ablation on actor observability and evaluate it in Section V by providing symbolic block color/orientation information to the actor in addition to critic feedback, demonstrating that such structured inputs can substantially improve learning stability and overall performance.

C. VLM Critic: Visual Execution Feedback

The critic is a VLM that observes task execution through visual snapshots and BT execution traces. Instead of estimating scalar rewards, it outputs structured natural-language feedback grounded in observable evidence. To support different stages of execution, the critic operates in three modes: *Initial*, *Intermediate*, and *Final*.

In addition to the textual critique, the critic outputs two scalars: an alarm score $s \in [0, 1]$ indicating issue severity, and a confidence $c \in [0, 1]$ indicating certainty. The alarm score is supervised using an ordinal severity rubric. In *Initial* mode we annotate $s=0.0$ for clean setup, $s \in [0.1, 0.3]$ for minor imperfections, $s \in (0.3, 0.5)$ for borderline cases, $s \in [0.5, 0.7]$ for actionable problems, and $s > 0.7$ for severe safety-critical issues. For *Intermediate/Final* (Human Alarm) annotations we use the same severity semantics but a slightly more tolerant rubric to account for inevitable manipulation noise, while preserving $s \geq 0.5$ as actionable problems and $s > 0.7$ as severe failures.

The VRL framework operates in an episodic closed loop. At each episode, the current BT is executed on the robot and the critic analyzes observations and traces to produce feedback. If $s \geq 0.5$ or $c < 0.3$, a human operator is notified. The actor then updates the BT using the final critic feedback and the real score. The overall procedure is summarized in Algorithm 1.

Algorithm 1: Verbal Reinforcement Learning (VRL)

Input: Initial Behavior Tree BT_0 , Actor \mathcal{A} , Critic \mathcal{C} **Output:** Refined Behavior Tree BT^* $BT \leftarrow BT_0$;Initialize actor memory $H \leftarrow \emptyset$;**for** $episode = 1$ to N **do** Reset critic episodic memory $M \leftarrow \emptyset$; Capture initial image I_0 ; $y_0 \leftarrow \mathcal{C}.INITIAL(I_0)$; **if** $ALARM(y_0)$ **then**

Notify human operator;

while $episode$ not terminated **do** Execute next subtree of BT ; Capture image I_t and BT trace T_t ; $y_t \leftarrow \mathcal{C}.INTERMEDIATE(I_t, T_t)$; **if** $ALARM(y_t)$ **then**

Notify human operator;

 Capture final image I_f and full trace T ; $F \leftarrow \mathcal{C}.FINAL(I_f, T)$; **if** $ALARM(F)$ **then**

Notify human operator;

 Collect RealScore R ; $BT \leftarrow \mathcal{A}(BT, F, R, H)$; $H \leftarrow H \cup \{F, R\}$;**return** BT ;

IV. EXPERIMENTAL SETUP

A. Robotic Platform

The experiments were conducted on a custom mobile manipulation robot designed to perform logistics tasks (Fig. 2).

The robot performs autonomous navigation between pre-defined zones and uses a vacuum gripper to pick, rotate and place blocks. The manipulation system allows handling up to a fixed batch size of four blocks per transport cycle.

B. Experimental Environment

We established certain specifications for the experimental field, including the existence of several load and unload zones, the designated starting area, and a movable object (shelf). For the purpose of experiments, we used the available robotics competition environment. (Fig. 3). The geometry of the field provides spatially distributed pickup and delivery zones suitable for warehouse-style manipulation tasks.

To imitate boxes, we are using wooden blocks of 150 mm x 50 mm x 30 mm. Two opposite large faces are painted in orange and blue, while the remaining faces are free of color. The upward facing color determines the orientation of the block. If the orange face faces upward, the block is incorrectly oriented (upside down).

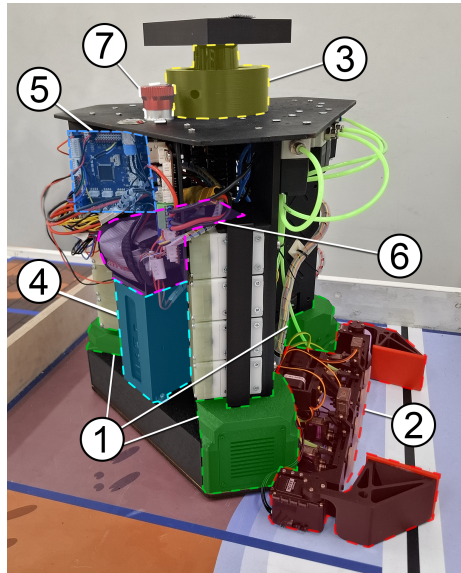


Fig. 2. Hardware architecture of the mobile robot: (1) three-wheeled omnidirectional base, (2) custom pneumatic gripper, (3) LiDAR sensor, (4) onboard Intel NUC computer, (5) custom STM32-based low-level controller, (6) LiPo battery, and (7) emergency stop button.

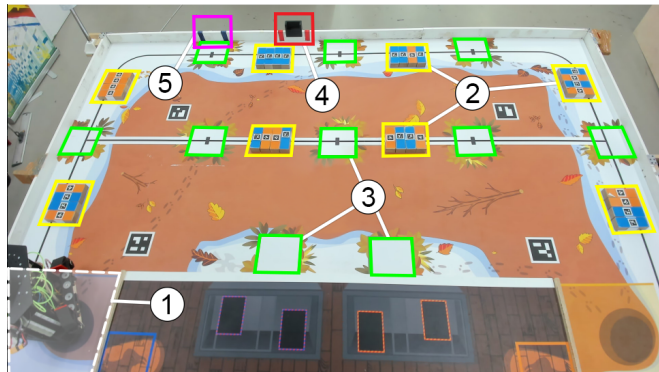


Fig. 3. Layout of the experimental environment: (1) start/finish area, (2) load zones containing block sets, (3) designated unload zones, (4) initial position of the movable shelf, and (5) target position of the movable shelf.

C. Task Definition

The experimental task represents a structured warehouse logistics scenario under a time constraint. The robot is required to transport blocks from load zones to unload zones. Blocks must be collected in batches of up to four units and placed such that each block is at least partially within an unload zone (i.e., any overlap/contact with the zone is sufficient). Each block must also be correctly oriented: the upward-facing colored side determines whether the placement is valid. In addition to block transportation, the robot must relocate a movable shelf along the boundary to the designated final side of the field. Successful relocation implicitly requires clearing adjacent zones, although this constraint is not explicitly encoded in the prompts. The episode is considered complete when the robot returns to

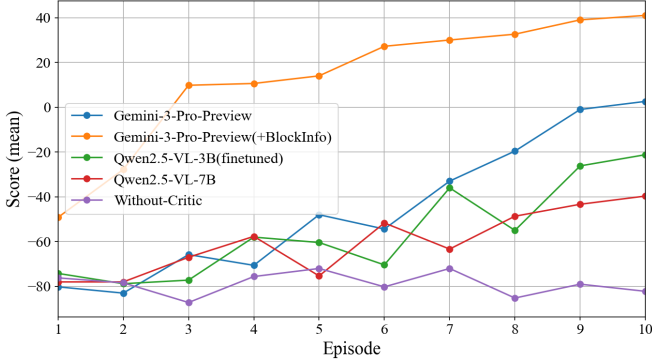


Fig. 4. Mean Score across environments.

the finish area.

We evaluate five distinct algorithmic configurations:

1. Without critic (BT Trace + real score only)
2. Qwen2.5 VL 7B Instruct
3. Qwen2.5 VL 3B Instruct (fine-tuned)
4. Gemini 3 Pro Preview (MLLM as critic)
5. Gemini 3 Pro Preview + block color information

To obtain the most objective and meaningful results, a series of experiments for each algorithm configuration were conducted on five different field configurations with varying block orientations. Ten training episodes were conducted for each field configuration, allowing for an objective assessment of training quality. Training was conducted in an episodic manner. After each episode, the actor updated the Behavior Tree using critic feedback and real score. Episodes were executed sequentially within each field configuration.

V. EXPERIMENTAL RESULTS

For each VLM, we report results averaged across all environment configurations. We analyze episodic learning behavior using four key metrics: score, critic accuracy, critic confidence, and human alarm rate. Together, these metrics characterize both the effectiveness of policy refinement and the reliability of visual feedback within the VRL framework.

The most important metric is episode score (Fig. 4). The episode score is computed according to a rule-based evaluation function that reflects task completion quality. The scoring scheme is designed to encourage structured logistics behavior and penalize operational errors. The scoring scheme is summarized in Table 1.

TABLE I
EPISODE SCORING RULES

Condition	Score
Operating time penalty	-1 point per second
Exceeding operating time limit	-20 points
Box correctly placed	+10 points per box
Full batch of 4 correctly placed blocks	+10 bonus points
Box incorrectly placed	-5 points per box
Box completely outside any zone	-10 points per box
Correct final robot position	+20 points

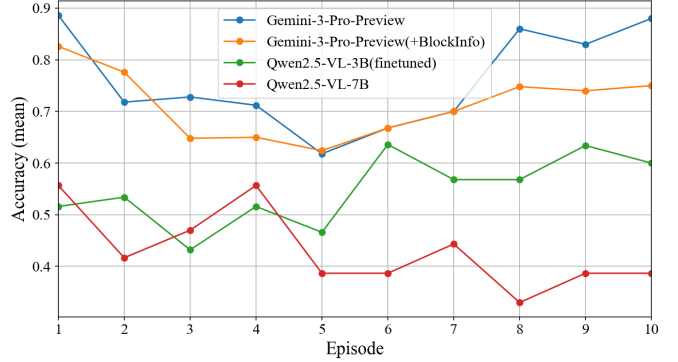


Fig. 5. Mean Accuracy across environments.

We first analyze the episodic score dynamics, which directly reflect task-level performance and successful policy refinement.

Our fine-tuned Qwen2.5-VL-3B model demonstrates more consistent and pronounced score improvement compared to the larger Qwen2.5-VL-7B model. Although the 3B variant has fewer parameters, it was fine-tuned on our structured execution-feedback dataset, which results in more grounded and task-relevant critiques during training. In contrast, the 7B model, used without task-specific adaptation, exhibits slower growth and higher variability. This indicates that domain adaptation is more critical than model scale for effective critic behavior in the VRL setting.

Next, we consider Gemini-3-Pro-Preview without additional symbolic inputs. This configuration achieves faster convergence and higher final scores than both Qwen variants, suggesting stronger inherent visual reasoning and feedback quality.

Providing structured block color information further improves learning stability and final performance. The Gemini (+BlockInfo) configuration achieves the highest score growth and the most stable convergence across episodes. This supports the hypothesis that structured symbolic perceptual inputs reduce ambiguity and enable more precise strategy-level corrections.

The baseline configuration without a critic demonstrates either extremely slow improvement or no consistent learning. Without structured visual feedback, the actor relies solely on scalar score signals, which are insufficient for diagnosing specific execution failures. As a result, policy refinement remains unstable and inefficient, highlighting the importance of critic-guided verbal reinforcement.

The second important metric is Accuracy (Fig. 5), which reflects how reliably the critic detects execution errors during task performance.

We quantify error detection performance using the Issue Detection Rate (IDR):

$$IDR = \frac{Detected\ Ground\ Truth\ Issues}{Real\ Ground\ Truth\ Issues}$$

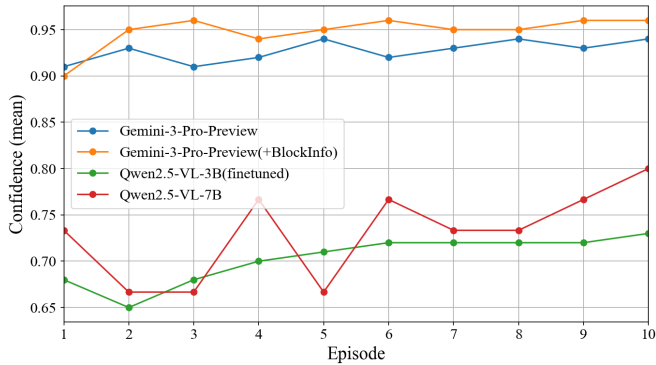


Fig. 6. Mean Confidence across environments.

This metric measures how consistently the critic identifies real execution problems observed in the scene.

Our fine-tuned Qwen2.5-VL-3B model demonstrates higher and more stable accuracy compared to the larger Qwen2.5-VL-7B model. Despite having fewer parameters, the domain-adapted 3B critic better captures task-specific failure modes, indicating that fine-tuning improves perceptual grounding and structured reasoning about execution errors.

The Qwen2.5-VL-7B model shows lower and more fluctuating accuracy across episodes, suggesting less consistent alignment between visual observations and task-relevant error categories.

Moving to Gemini-3-Pro-Preview, we observe substantially higher detection accuracy compared to both Qwen variants. The model demonstrates strong visual grounding and reliable identification of incorrectly placed or misoriented blocks across most episodes.

When additional symbolic block color information is provided, the Gemini (+BlockInfo) configuration maintains consistently strong detection performance across episodes. The structured perceptual abstraction reduces ambiguity in orientation interpretation and supports more stable error identification throughout the learning process.

In the absence of a critic, no explicit error detection mechanism exists. Consequently, the system cannot localize execution failures, which explains the unstable and slow policy improvement observed in the score analysis.

The next key metric is Confidence (Fig. 6), which reflects how certain the critic is about its assessments during execution. While accuracy measures correctness, confidence provides insight into calibration and reliability of the critic’s judgments.

The fine-tuned Qwen2.5-VL-3B model demonstrates more stable confidence levels across episodes compared to the larger Qwen2.5-VL-7B model. The 3B critic maintains moderate but consistent confidence, suggesting improved calibration after task-specific fine-tuning. In contrast, the 7B model exhibits higher variance in confidence, indicating less stable alignment between visual observations and internal

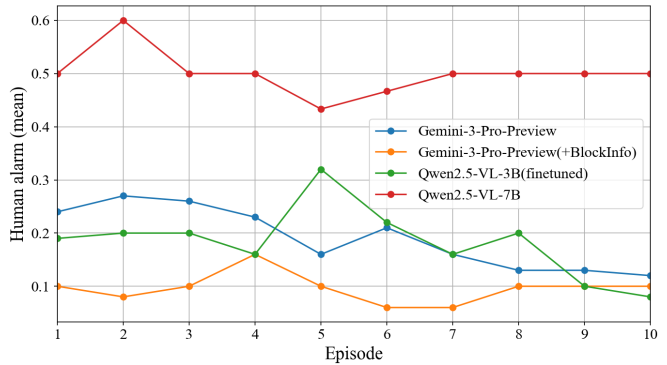


Fig. 7. Mean Human Alarm across environments.

reasoning.

The Gemini-3-Pro-Preview critic maintains generally high confidence throughout training, reflecting strong visual grounding capabilities. However, without structured block information, confidence occasionally remains high even in early episodes where planning errors are frequent.

When block color information is provided, Gemini (+BlockInfo) shows both high and more consistent confidence. The additional symbolic input appears to reduce perceptual ambiguity, leading to more calibrated and stable certainty levels.

In the absence of a critic, confidence cannot be meaningfully defined, as no structured assessment of execution is produced. This further highlights the importance of a calibrated critic for stable verbal reinforcement learning.

The final metric is Human Alarm (Fig. 7), which measures how often the critic triggers a safety or execution alert requiring human attention. This signal reflects both error detection reliability and safety awareness during task execution.

Fine-tuned Qwen2.5-VL-3B critic shows a gradual decrease in alarm frequency across episodes. As policy quality improves and execution errors become less frequent, the number of triggered alarms correspondingly declines. This indicates that the critic adapts well to the evolving task performance and does not over-trigger unnecessary alerts.

In contrast, Qwen2.5-VL-7B produces a higher and more variable alarm rate. The instability suggests weaker calibration and less consistent distinction between critical failures and minor execution imperfections.

The Gemini-3-Pro-Preview critic demonstrates a more stable alarm profile, with relatively high alarm rates during early episodes followed by a steady reduction as the policy improves. This behavior is desirable, as it reflects sensitivity to genuine failures during exploration while avoiding excessive intervention later.

The Gemini (+BlockInfo) configuration achieves the most balanced alarm behavior. Early alarms correctly capture orientation and placement errors, while later episodes show a significant reduction in unnecessary alerts. The structured perceptual input improves both detection precision and safety

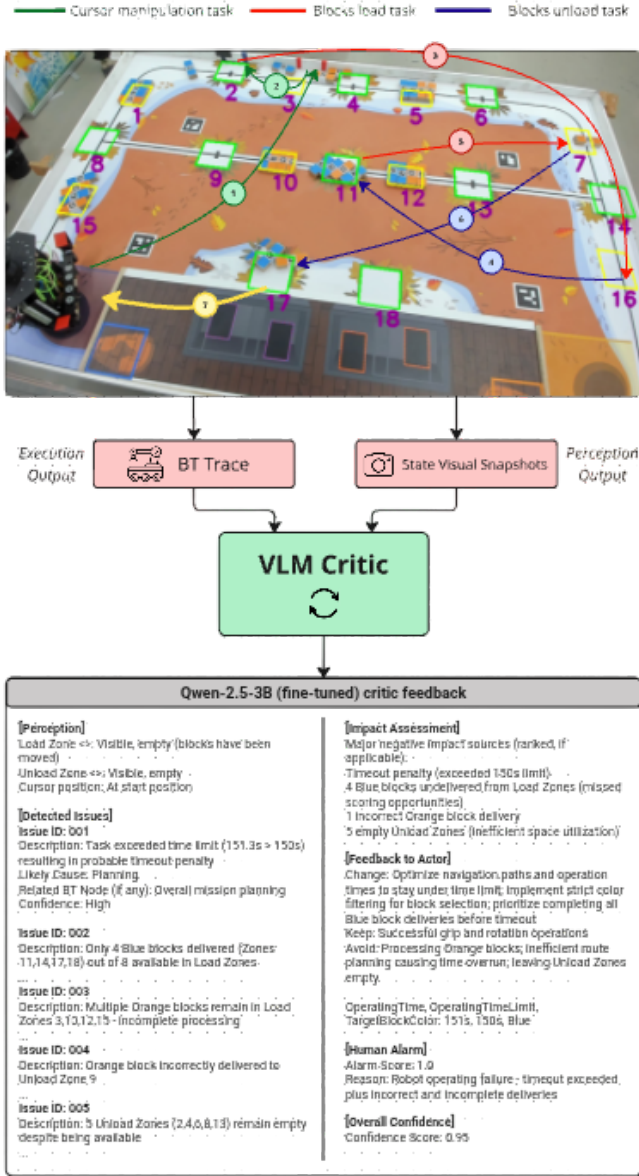


Fig. 8. Episode of the Qwen2.5-VL-3B (fine-tuned) critic.

calibration.

Finally, in the absence of a critic, no alarm mechanism exists. As a result, execution failures are not explicitly flagged, and the learning process a safety-aware feedback channel. This further supports the importance of critic-driven structured supervision within the VRL framework.

Particular attention is given to a representative episode of the Qwen2.5-VL-3B (fine-tuned) critic. In Fig. 8, we show the full robot trajectory during the task, together with the intermediate visual inputs processed by the VLM and the corresponding critic feedback. Based on the structured output of the fine-tuned critic, the system correctly identifies the key failure in the episode and, importantly, attributed it to

Before (rotation + decoupled retries)

```

<Sequence>
  <RetryUntilSuccessful num_attempts="2">
    <SubTree ID="CursorSequence"/>
  </RetryUntilSuccessful>
  <RetryUntilSuccessful num_attempts="2">
    <Sequence>
      <Action ID="MoveToZone" zone="1" position="1" />
    <SubTree ID="LoadBlocksSequence"/>
  </RetryUntilSuccessful>
  <Sequence>
    <Action ID="RotateBlocks" mask="1111" />
    <CustomDelay duration="3.0"/>
  </Sequence>
  <RetryUntilSuccessful num_attempts="2">
    <Sequence>
      <Action ID="MoveToZone" zone="2" />
    <SubTree ID="UnloadBlocksSequence"/>
  </RetryUntilSuccessful>
  ...[3->4, 5->6, 7->8, 8->Home]
</Sequence>

```

After (transactional retries, no rotations)

```

<Sequence>
  <RetryUntilSuccessful num_attempts="2">
    <Sequence>
      <SubTree ID="CursorSequence"/>
    </Sequence>
  </RetryUntilSuccessful>
  <RetryUntilSuccessful num_attempts="2">
    <Sequence>
      <Action ID="MoveToZone" zone="1" position="1" />
    <SubTree ID="LoadBlocksSequence"/>
    <Action ID="MoveToZone" zone="2" position="1" />
    <SubTree ID="UnloadBlocksSequence"/>
  </Sequence>
  ...[3->4, 5->6, 7->8]
</RetryUntilSuccessful num_attempts="2">
  <Sequence>
    <Action ID="MoveToHome"/>
  </Sequence>
</RetryUntilSuccessful>
</Sequence>

```

Removed/Changed (pink) Added (green)

Fig. 9. Qualitative BT evolution under perceptual uncertainty.

the appropriate Impact Issue category and related BT node. This precise classification allows the actor to understand not only that an error occurred, but how it affected overall task planning and execution. Such impact-aware attribution is essential for targeted correction rather than global, unfocused replanning.

In comparison, the unfine-tuned Qwen2.5-VL-7B critic tends to produce high-level feedback with weaker calibration and limited spatial grounding. Fine-tuning improves task relevance and consistency of confidence, although it may reduce perceptual breadth. More generally, while strong multimodal critics are effective at problem classification and causal understanding, they may over-focus on local perceptual details at the expense of global efficiency. In our case, the actor implicitly adapts to the critic’s characteristics, adjusting its strategy in response to the type and structure of feedback it receives. This behavior indicates the emergence of critic-aware planning, where policy updates are shaped not only by task rewards but also by the critic’s perceptual and diagnostic biases.

A. Qualitative BT evolution under perceptual uncertainty

To complement the aggregate learning curves, Fig. 9 illustrates a representative refinement step where the critic’s perceptual grounding is insufficient for reliable color/orientation reasoning. In this episode, the critic reports empty unload zones and flags a generic execution failure, whereas the BT trace and RealScore indicate successful transport and placement. The actor therefore treats the critic output as a noisy hypothesis and grounds the update in trace- and score-evidence, applying a conservative and interpretable BT patch: (i) disabling the blind RotateBlocks (mask=1111) routine to avoid time overhead and accidental mis-rotations when color perception is unreliable; (ii) fixing an execution-engine edge case by wrapping CursorSequence inside a Sequence under RetryUntilSuccessful; and (iii) restructuring the policy into isolated transac-

tional Load--Transport--Unload subtrees wrapped with `RetryUntilSuccessful`, preventing macro-retries across multiple zone pairs. This behavior also motivates our `BlockInfo` ablation, where reliable symbolic color/orientation estimates enable re-introducing targeted rotations and improve convergence.

VI. DISCUSSION

The experimental results indicate that critic alignment with the task domain plays a more significant role than raw model scale. Although `Qwen2.5-VL-3B` contains fewer parameters than the 7B variant, the fine-tuned 3B model demonstrates more stable learning dynamics and stronger score improvement. This suggests that adaptation to structured execution feedback and alignment with Behavior Tree-level error categories are more important than generic visual capacity. The larger untuned model retains broader visual knowledge but lacks tight alignment with the symbolic planning abstraction, resulting in less consistent and less actionable critiques.

`Gemini-3-Pro-Preview` achieves stronger overall performance, which can be attributed to higher-quality visual grounding and more robust spatial reasoning. The task requires resolving fine-grained spatial relationships, such as identifying block orientation from colored faces, verifying full containment within unload zones, and detecting shelf displacement along field boundaries. Small perceptual errors directly translate into discrete symbolic consequences at the planning level. In particular, accurate recognition of the movable shelf position along the boundary is critical, since even minor misalignment affects the validity of task completion. Gemini’s stronger multimodal reasoning enables more precise and consistent error detection, which in turn enables more effective Behavior Tree refinement. When additional symbolic block color information is provided, perceptual ambiguity is further reduced, shifting the burden from low-level visual inference to structured reasoning. This explains the increased stability and higher final performance of the Gemini (+`BlockInfo`) configuration.

At the same time, the performance gap between models is not extreme. Once critic accuracy surpasses a sufficient reliability threshold, additional perceptual improvements mainly affect convergence speed rather than ultimate policy structure. Because the actor operates in a constrained symbolic space defined by executable Behavior Trees, the magnitude of possible updates is inherently bounded. Therefore, improvements in critic quality yield diminishing returns beyond a certain level of perceptual reliability.

An additional observation is that the actor appears to adapt implicitly to the critic’s limitations. This effect is illustrated in Fig. 9, where the actor disables perception-sensitive rotations and prioritizes throughput when the critic cannot reliably ground color/zone evidence.

Since policy updates are driven by structured verbal feedback, the actor gradually internalizes which types of failures are reliably detected and which signals are unstable or ambiguous. This induces a form of co-adaptation: the critic defines the informational structure of the learning signal, and

the actor adjusts its strategy refinement accordingly. As a result, learning remains relatively stable even when critic feedback is imperfect, which explains why weaker models degrade performance gradually rather than catastrophically.

Despite these strengths, the system’s performance remains fundamentally constrained by what the critic can observe and attribute within its limited temporal context. The current VRL formulation assumes that relevant faults are visible within the critic’s snapshot-based window and can be causally linked to recent BT events. Detecting latent faults with delayed consequences remains challenging, as errors may only manifest several steps later, outside the immediate observation context. Addressing this limitation likely requires longer-horizon temporal reasoning and more explicit trace-aware root-cause attribution.

A second limitation is that VRL inherits the critic’s perceptual reliability. When the critic is insufficiently adapted, perceptual mismatches can yield incorrect causal hypotheses. As shown in Fig. 9, the actor can mitigate this by adopting conservative updates that reduce reliance on uncertain perceptual cues, but this may trade off optimality (e.g., disabling rotations that could be beneficial under reliable color observation). Improving critic grounding and incorporating explicit uncertainty handling or structured perceptual inputs (`BlockInfo`) are important directions.

Overall, these findings support the central premise of the proposed framework: effective task-level reinforcement in physical robotics does not rely on end-to-end differentiable policy learning, but rather reliable, structured, and well-aligned verbal feedback grounded in observable execution outcomes. At the same time, they highlight that further improvements in critic grounding, temporal reasoning, and structured feedback design are key directions for advancing Verbal Reinforcement Learning in real-world robotic systems.

VII. CONCLUSION

We presented a closed-loop Verbal Reinforcement Learning (VRL) framework for task-level policy refinement in mobile robotics. VRL addresses the problem of execution uncertainty in stochastic real-world settings by combining a VLM-based critic with an LLM-based actor. The critic generates structured natural-language feedback based on robot observations, allowing the actor to iteratively refine Behavior Trees without gradient-based optimization.

Key findings from experiments with physical robots include:

1. Numerical rewards alone are ineffective under uncertainty, as they cannot distinguish execution (hardware) errors from planning errors. Structured feedback is essential for stable policy improvement.
2. The quality of causal attribution is more important than perceptual accuracy. A critic that correctly diagnoses the causes of failures ensures robust adaptation even with imperfect object detection.
3. Structured perceptual inputs accelerate convergence,

demonstrating that the main bottleneck of VRL is the perceptual foundation, not symbolic planning.

VRL enables interpretable, hardware-based policy adaptation in the real world—without simulators or gradients. Performance depends on the accuracy of the critic and the design of the hints, but this framework suggests a promising direction toward transparent robot learning that accounts for the gap between plan and reality.

REFERENCES

- [1] V. Malathi, P. Sreedharan, R. P. R., V. A. Kumar, A. L. Sadasivan, G. Udupa, L. Pastorelli, and A. Troppina, “Decision-making for path planning of mobile robots under uncertainty: A review of belief-space planning simplifications,” *Robotics*, vol. 14, no. 9, p. 127, 2025.
- [2] S. Thrun, W. Burgard, and D. Fox, *Probabilistic Robotics*. MIT Press, 2005. [Online]. Available: <https://mitpress.mit.edu/9780262201629/probabilistic-robotics/>
- [3] E. Scheide, G. Best, and G. A. Hollinger, “Behavior tree learning for robotic task planning through monte carlo dag search over a formal grammar,” in *Proc. IEEE Int. Conf. Robotics and Automation (ICRA)*, 2021, pp. 4837–4843.
- [4] M. Colledanchise and P. Ögren, “How behavior trees modularize hybrid control systems and generalize sequential behavior compositions, the subsumption architecture, and decision trees,” *IEEE Trans. Robotics*, vol. 33, no. 2, pp. 372–389, 2017.
- [5] D. Amodei, C. Olah, J. Steinhardt, P. Christiano, J. Schulman, and D. Mané, “Concrete problems in ai safety,” 2016, arXiv:1606.06565.
- [6] B. Ichter, A. Brohan, Y. Chebotar, C. Finn, K. Hausman, A. Herzog, D. Ho, J. Ibarz, A. Irpan, E. Jang, *et al.*, “Do as i can, not as i say: Grounding language in robotic affordances,” in *Proc. 6th Conf. Robot Learning (CoRL)*, ser. Proceedings of Machine Learning Research, vol. 205, 2023, pp. 287–318.
- [7] J. Liang, W. Huang, F. Xia, P. Xu, K. Hausman, B. Ichter, P. Florence, and A. Zeng, “Code as policies: Language model programs for embodied control,” in *Proc. IEEE Int. Conf. Robotics and Automation (ICRA)*, 2023, pp. 9493–9500.
- [8] I. Singh, V. Blukis, A. Mousavian, *et al.*, “Progprompt: Program generation for situated robot task planning using large language models,” *Autonomous Robots*, vol. 47, pp. 999–1012, 2023.
- [9] T. Birr, C. Pohl, A. Younes, and T. Asfour, “Autogpt+*p*: Affordance-based task planning using large language models,” in *Proc. Robotics: Science and Systems (RSS)*, 2024.
- [10] N. Shinn, F. Cassano, A. Gopinath, K. Narasimhan, and S. Yao, “Reflection: Language agents with verbal reinforcement learning,” in *Proc. 37th Int. Conf. Neural Information Processing Systems (NeurIPS)*, New Orleans, LA, USA, 2023, p. Art. no. 377.
- [11] S. Yao, J. Zhao, D. Yu, I. Shafraan, K. R. Narasimhan, and Y. Cao, “React: Synergizing reasoning and acting in language models,” in *Proc. NeurIPS 2022 Foundation Models for Decision Making Workshop*, 2022.
- [12] A. Madaan, N. Tandon, P. Gupta, S. Hallinan, L. Gao, S. Wiegreffe, U. Alon, N. Dziri, S. Prabhume, Y. Yang, S. Gupta, B. P. Majumder, K. Hermann, S. Welleck, A. Yazdanbakhsh, and P. Clark, “Self-refine: Iterative refinement with self-feedback,” in *Proc. 37th Int. Conf. Neural Information Processing Systems (NeurIPS)*, New Orleans, LA, USA, 2023, p. Art. no. 2019.
- [13] W. Huang, C. Wang, R. Zhang, Y. Li, J. Wu, and L. Fei-Fei, “Voxposer: Composable 3d value maps for robotic manipulation with language models,” in *Proc. 7th Annu. Conf. Robot Learning (CoRL)*, 2023. [Online]. Available: <https://doi.org/10.48550/arXiv.2307.05973>
- [14] Y. Ding, X. Zhang, C. Paxton, and S. Zhang, “Task and motion planning with large language models for object rearrangement,” in *Proc. IEEE/RSJ Int. Conf. Intelligent Robots and Systems (IROS)*, Detroit, MI, USA, 2023, pp. 2086–2092.
- [15] W. Huang, F. Xia, T. Xiao, H. Chan, J. Liang, P. Florence, A. Zeng, J. J. R. Tompson, I. Mordatch, Y. Chebotar, *et al.*, “Innermonologue: Embodied reasoning through planning with language models,” in *Proc. Conf. Robot Learning (CoRL)*, 2022, to appear. [Online]. Available: <https://innermonologue.github.io/>
- [16] A. Lykov, M. Dronova, N. Naglov, M. Litvinov, S. Satevich, A. Bazhenov, V. Berman, A. Shcherbak, and D. Tsetsrukou, “Llm-mars: Large language model for behavior tree generation and nlp-enhanced dialogue in multi-agent robot systems,” 2023, arXiv:2312.09348.
- [17] S. Liu, J. Zhang, R. X. Gao, X. V. Wang, and L. Wang, “Vision-language model-driven scene understanding and robotic object manipulation,” in *Proc. IEEE 20th Int. Conf. Automation Science and Engineering (CASE)*, 2024, pp. 21–26.
- [18] J. Wang, E. Shi, H. Hu, C. Ma, Y. Liu, X. Wang, Y. Yao, X. Liu, B. Ge, and S. Zhang, “Large language models for robotics: Opportunities, challenges, and perspectives,” *Journal of Automation and Intelligence*, vol. 4, no. 1, pp. 52–64, 2025.
- [19] G. Wang, Y. Xie, Y. Jiang, A. Mandlekar, C. Xiao, Y. Zhu, L. Fan, and A. Anandkumar, “Voyager: An open-ended embodied agent with large language models,” *Trans. Mach. Learn. Res.*, 2024.
- [20] R. A. Izzo, G. Bardaro, and M. Matteucci, “Btgenbot: Behavior tree generation for robotic tasks with lightweight llms,” in *Proc. IEEE/RSJ Int. Conf. Intelligent Robots and Systems (IROS)*, 2024, pp. 9684–9690.
- [21] Y. Wang, Z. Sun, J. Zhang, Z. Xian, E. Biyik, D. Held, and Z. Erickson, “Rl-vlm-f: Reinforcement learning from vision language foundation model feedback,” in *Proc. 41st Int. Conf. Machine Learning (ICML)*, Vienna, Austria, 2024, p. Art. no. 2112.
- [22] J. Rocamonde, V. Montesinos, E. Nava, E. Perez, and D. Lindner, “Vision-language models are zero-shot reward models for reinforcement learning,” in *Proc. 12th Int. Conf. Learning Representations (ICLR)*, 2024.
- [23] A. Singh, A. Bhaskar, P. Yu, S. Chakraborty, R. Dasyam, A. S. Bedi, and P. Tokekar, “Varp: Reinforcement learning from vision-language model feedback with agent regularized preferences,” 2025, arXiv:2503.13817.
- [24] X. Dang and S. Edelkamp, “Clip-motion: Learning reward functions for robotic actions using consecutive observations,” 2025, arXiv:2311.03485.
- [25] Y. Zeng, Y. Mu, and L. Shao, “Learning reward for robot skills using large language models via self-alignment,” in *Proc. 41st Int. Conf. Machine Learning (ICML)*, Vienna, Austria, 2024, p. Art. no. 2408.
- [26] O. Y. Lee, A. Xie, K. Fang, K. Pertsch, and C. Finn, “Affordance-guided reinforcement learning via visual prompting,” in *Proc. IEEE/RSJ Int. Conf. Intelligent Robots and Systems (IROS)*, Hangzhou, China, 2025, pp. 2352–2359.
- [27] L. Guan, Y. Zhou, D. Liu, Y. Zha, H. B. Amor, and S. Kambhampati, “Task success is not enough: Investigating the use of video-language models as behavior critics for catching undesirable agent behaviors,” in *Proc. First Conf. Language Modeling*, 2024.